Cell. Mol. Life Sci. (2015) 72:2949–2960
DOI 10.1007/s00018-015-1877-3

Cellular and Molecular Life Sciences

RESEARCH ARTICLE

Senescence of human skin-derived precursors regulated by Akt-FOXO3-p27^{KIP1}/p15^{INK4b} signaling

Shuang Liu · Xinyue Wang · Qian Zhao · Shu Liu · Huishan Zhang · Junchao Shi · Na Li · Xiaohua Lei · Huashan Zhao · Zhili Deng · Yujing Cao · Lina Ning · Guoliang Xia · Enkui Duan

Received: 15 January 2015 / Revised: 26 February 2015 / Accepted: 27 February 2015 / Published online: 10 March 2015

Abstract Multipotent skin-derived precursors (SKPs) are dermal stem cells with the capacity to reconstitute the dermis and other tissues, such as muscles and the nervous system. Thus, the easily available human SKPs (hSKPs) hold great promises in regenerative medicine. However, long-term expansion is difficult for hSKPs in vitro. We previously demonstrated that hSKPs senesced quickly under routine culture conditions. To identify the underlying mechanisms so as to find an effective way to expand hSKPs, time-dependent microarray analysis of gene expression in hSKPs during in vitro culture was performed. We found that the senescence of hSKPs had a unique gene expression pattern that differs from reported typical senescence. Subsequent investigation ruled out the role of DNA damage and classical p53 and p16^{INK4a} signaling in hSKP senescence. Examination of cyclin-dependent kinase inhibitors revealed the involvement of p15^{INK4b} and p27^{KIP1}. Further exploration about upstream signals indicated the contribution of Akt hypo-activity and FOXO3 to hSKP senescence. Forced activation of Akt and knockdown of FOXO3, p15^{INK4b} and p27^{KIP1} effectively inhibited hSKP senescence and promoted hSKP proliferation. The unique senescent phenotype of human dermal stem cells and the role of Akt-FOXO3-p27^{KIP1}/p15^{INK4b} signaling in regulating hSKP senescence provide novel insights into the senescence and self-renewal regulation of adult stem cells. The present study also points out a way to propagate hSKPs in vitro so as to fulfill their promises in regenerative medicine.

Keywords Cellular senescence · Skin-derived precursors · Akt · p15^{INK4b} · p27^{KIP1} · Adult stem cells

Abbreviations

CDKI	Cyclin-dependent kinase inhibitor
DDR	DNA damage response
DSB	Double strand break
MAPK	Mitogen-activated protein kinase
NF-κB	Nuclear factor kappa-light-chain-enhancer of activated B cells
PCNA	Proliferating cell nuclear antigen
PI3K	Phosphatidylinositol-4,5-bisphosphate 3-kinase
RB	Retinoblastoma protein
SASP	The senescence-associated secretory phenotype
SIPS	Stress-induced premature senescence
SKPs	Skin-derived precursors

S. Liu, X. Wang and Q. Zhao contributed equally to this work.

Electronic supplementary material The online version of this article (doi:10.1007/s00018-015-1877-3) contains supplementary material, which is available to authorized users.

S. Liu · X. Wang · S. Liu · H. Zhang · J. Shi · N. Li · X. Lei · H. Zhao · Z. Deng · Y. Cao · L. Ning · E. Duan (✉)
State Key Laboratory of Reproductive Biology, Institute of Zoology, Chinese Academy of Sciences, 1 Beichen West Road, Chaoyang District, Beijing 100101, China
e-mail: duane@ioz.ac.cn

Q. Zhao · G. Xia (✉)
State Key Laboratory of Agrobiotechnology, College of Biological Sciences, China Agricultural University, No. 2 Yuanmingyuan Xilu, Haidian District, Beijing 100193, China
e-mail: glxiachina@sohu.com

J. Shi · N. Li · H. Zhao · Z. Deng
University of Chinese Academy of Sciences, Beijing 100049, China

Introduction

One of the fascinating characters of human adult stem cells is their ability to develop into the whole tissue, which holds great promises in regenerative medicine. Of all human adult stem cells, skin-derived stem cells are of special interests because of their easy availability [1]. Skin-derived precursors (SKPs) are multipotent stem cells enriched from the mammalian dermis. Their capacity to regenerate all the dermal cell types makes them useful in skin wound healing and hair follicle reconstitution [2]. Moreover, additional differentiation potential of SKPs has been revealed. Rodent SKPs are capable of repairing damaged muscles, bones, as well as the nervous system [3–5]. Although human SKPs (hSKPs) can be isolated with similar protocols, their long-term expansion in vitro is defective [6, 7]. We previously demonstrated that foreskin-derived adult hSKPs senesced quickly in vitro, which could be partially alleviated by enhancing PI3K-Akt pathway activity or culturing hSKPs with micro-environment-mimicking three-dimensional hydrogel scaffolds [8, 9]. To realize the therapeutic potential of hSKPs, further inhibition of their senescence and the promotion of their propagation are of great significance.

Cellular senescence is a state of irreversible cell cycle arrest triggered by multiple insults. Replicative senescence often occurs after many cell doublings when the telomere was shortened to critical minimal length to trigger the DNA damage response (DDR) [10]. Cellular senescence can also been induced prematurely by oncogene activation, inadequate culture conditions, oxidative stress, as well as ultraviolet and ionizing radiation [11]. Physiologically, senescence is regarded as a tumor-suppressing mechanism [11]. For many cell types, stress-induced premature senescence (SIPS), rather than apoptosis, is how cells respond to sub-cytotoxic levels of stresses, both in vitro and in vivo [12]. Thus, it is of great importance to reveal the mechanisms underlying SIPS, especially for adult stem cells that are prone to be subject to environmental insults, such as skin- and intestine-resident stem cells.

It is well demonstrated that p53-$p21^{CIP1}$ and $p16^{INK4a}$-pRB signal cascades are the two most common and important senescence-mediating pathways which finally led to the cell cycle arrest at the G1 phase. Many upstream signals are reported to exert in cellular senescence, such as PI3K-Akt, p38 MAPK, and NF-κB signals [13–15]. We previously found that PI3K-Akt pathway inhibits the senescence of hSKPs while promoting their self-renewal [8]. To further dissect relevant mechanisms of hSKP senescence, we investigated the time-dependent gene expression profiles of hSKPs in culture. Surprisingly, the senescence of hSKPs displayed distinct gene expression pattern from known classical senescent phenotype. Further exploration of related signals also revealed mechanisms other than p53 and $p16^{INK4a}$ signaling. With gain- and loss-of-function studies, we demonstrated that the senescence of hSKPs was mediated by the Akt-FOXO3-$p27^{KIP1}$/$p15^{INK4b}$ signaling. The unique characteristics and specialized mechanism of hSKP senescence provide novel insights into the senescence and self-renewal control of adult stem cells. The present study also points out a way to propagate hSKPs so as to fulfill their promises in regenerative medicine.

Materials and methods

Plasmids and construction of lentiviral vectors

Foxo3, *Cdkn1b* and *Cdkn2b* lentiviral shRNA vectors were purchased from TRC Lentiviral shRNA Libraries (Thermo), and the backbone vector was pLKO.1. *Cdkn2a* and *Tp53* lentiviral shRNA vectors, which were also constructed into pLKO.1, were kind gifts from Prof. Zengqiang Yuan at the Institute of Biophysics, Chinese Academy of Sciences. pLKO.1 containing a scramble sequence with no specific target was used as a negative control in all RNA interference (RNAi) experiments.

901 pLNCX Myr HA Akt1 and 902 pLNCX Myr HA Akt1 K179M plasmids were purchased from Addgene (http://www.addgene.org). The myr HA Akt1 and myr HA Akt1 K179M sequences were cloned using PCR with a forward primer "5′-CCGCTCGAGATGGGGTCTTCAAAATCTA A-3′" and a reverse primer "5′-GGAATTCAGGCCGTGC CGCTGGCCG-3′". Interested sequences were cloned into a lentiviral vector pLVX-AcGFP1-N1 (Cat# 632154 Clontech). The empty pLVX-AcGFP1-N1 vector with GFP was used as a parallel control to monitor transfection efficiency.

Skin sample processing and initial hSKP and hFb culture

Human foreskin samples were derived from voluntary circumcisions with informed consents. The protocol was approved by the Ethics Committee of the Institute of Zoology, Chinese Academy of Sciences. The foreskin sample processing and cell isolation procedures were described previously [8]. Briefly, fresh foreskin samples were washed, and subcutaneous tissues were removed. After overnight incubation in 5 mg/ml Dispase (Cat# 17105-041 Gibco), dermis were collected and further digested with Collagenase Type IV (Cat# 17104-019 Gibco) into liquid form. Single dermal cells were harvested, washed, plated at a density of 10^6 cells/ml into non-tissue-culture-treated petri dishes (Cat#351029 BD Falcon) and finally cultured at 37 °C with 5 % CO_2. The hSKP

culture medium was DMEM/F12 (Cat# 11320-033 Gibco) with 20 ng/ml epidermal growth factor (EGF, Cat# AF-100-15 PeproTech, NJ, USA), 40 ng/ml basic fibroblast growth factor (bFGF, Cat# AF-100-18b PeproTech) and 2 % B27 (Cat# 12587-010 Gibco). hSKPs formed spheres via proliferation and aggregation in suspension culture. After Day 3, cells were cultured in poly-HEMA (Cat# P3932 Sigma) coated petri dishes to prohibit attachment. hFbs were cultured by plating freshly isolated dermal cells on tissue-culture-treated 10-cm dishes (Cat# 430166 Corning). The culture medium was DMEM (Cat# 10569010 Gibco) with 10 % fetal bovine serum (FBS, Cat# SH30084.03 Hyclone).

Sub-culture and treatments of hSKPs

Routinely, the culture medium was changed every 3 days by centrifugation, and SKP spheres were trypsinized into single cells with 0.25 % trypsin (Cat# 25200056 Gibco) every 6 days. In certain experiments, hSKPs were treated with different factors or transduced with lentiviral vectors. For growth factor and chemical compound treatments, Day 3 hSKPs were treated with different concentrations and combinations of growth factors or chemical compounds. Cells were trypsinized on Day 6; the medium was changed on Day 9 and cells were harvested for analysis on Day 12 unless specifically indicated otherwise.

For lentiviral transduction, Day 3 hSKPs were trypsinized into single cells and forced to adhere to a tissue-culture-treated 10-cm dish (Corning) at a density of 2×10^6 cells/dish by adding 5 % FBS (Hyclone). 7 h after cell plating, lentiviruses were added to the culture medium with 8 μg/ml polybrene (Cat# H9268 Sigma). Cells were trypsinized 24 h after transduction and cultured in suspension as usual without FBS. Cells were harvested on Day 13.

Cell harvest for subsequent analysis

On the day of cell harvest, hSKP spheres were collected by centrifugation. In some cases, hSKP spheres were cytospinned directly for staining. In other cases, such as flow cytometry or quantitative analysis of staining, hSKP spheres were trypsinized into single cells and washed in PBS before being processed. For subsequent RNA purification or protein collection, hSKPs spheres were also trypsinized and washed to achieve better cell dissociation.

More detailed experimental procedures for lentivirus production, immunostaining, flow cytometry and so on are presented in the supplementary experimental procedures.

Results

Characterization of the senescent phenotype of hSKPs

We previously reported that hSKPs quickly senesced in culture. Here, we further examined the detailed phenotype of hSKPs. Adherent hSKPs from early and late passages exhibited evident differences in morphology. Day 24 attached cells were larger, flatter and more irregular in shape than Day 3 attached cells (Fig. 1a). Also, Day 24 hSKP spheres showed uniformly intense SA-β-gal staining, whereas only a variable small portion of freshly isolated dermal cells were SA-β-gal+ (Fig. 1b). There was no connection between the donor age and the SA-β-gal staining of Day 0 dermal cells (Fig. S1).

The decrease of hSKP proliferation was previously revealed by Ki67 staining [8]. Here, the proliferation decline and G1 cell cycle arrest of hSKPs were further demonstrated by the down-regulation of proliferating cell nuclear antigen (PCNA) expression and RB phosphorylation at Ser807/811 (Fig. 1c, d). Ki67 and phosphorylated RB (p-RB) did not necessarily co-exist in the same cells, but there were cells expressing both proteins (Fig. 1e). The relationship between Ki67+ proliferating cells and SA-β-gal+ senescent cells was also investigated. Intriguingly as indicated in Fig. 1f, Ki67 and SA-β-gal staining was not strictly exclusive. A few Ki67+ cells also showed some degree of SA-β-gal staining, possibly due to incomplete growth arrest.

Changes in gene expression during hSKP senescence

To further understand the mechanisms underlying hSKP senescence, hSKPs of two independent cultures that had comparable senescence rate (designated as A and B) were collected on Day 3, 6, 9 and 12, and time-dependent microarray analysis was performed (Fig. 2a). The sampling protocol is shown in Fig. S2. Complete gene expression data are presented in Table S1. Sample clustering analysis based on overall gene expression showed that Day 9 and 12 hSKPs were similar in gene expression pattern, and had more differential gene expression compared with Day 3 cells, consistent with the SA-β-gal staining results (Fig. 2b). However, Day 6 cells from Sample A were more similar to Day 9 and 12 cells, whereas those from Sample B were more like Day 3 cells, indicating that Sample A and B still exhibited slight variance in senescent rate. Overall gene expression changed most dramatically during Day 3 and 9, corresponding to the quick increase in SA-β-gal activity during this period (Fig. 2a).

With a Short Time-series Expression Miner software [16], genes whose expression changed ≥2 fold and had significant change patterns during culture were identified

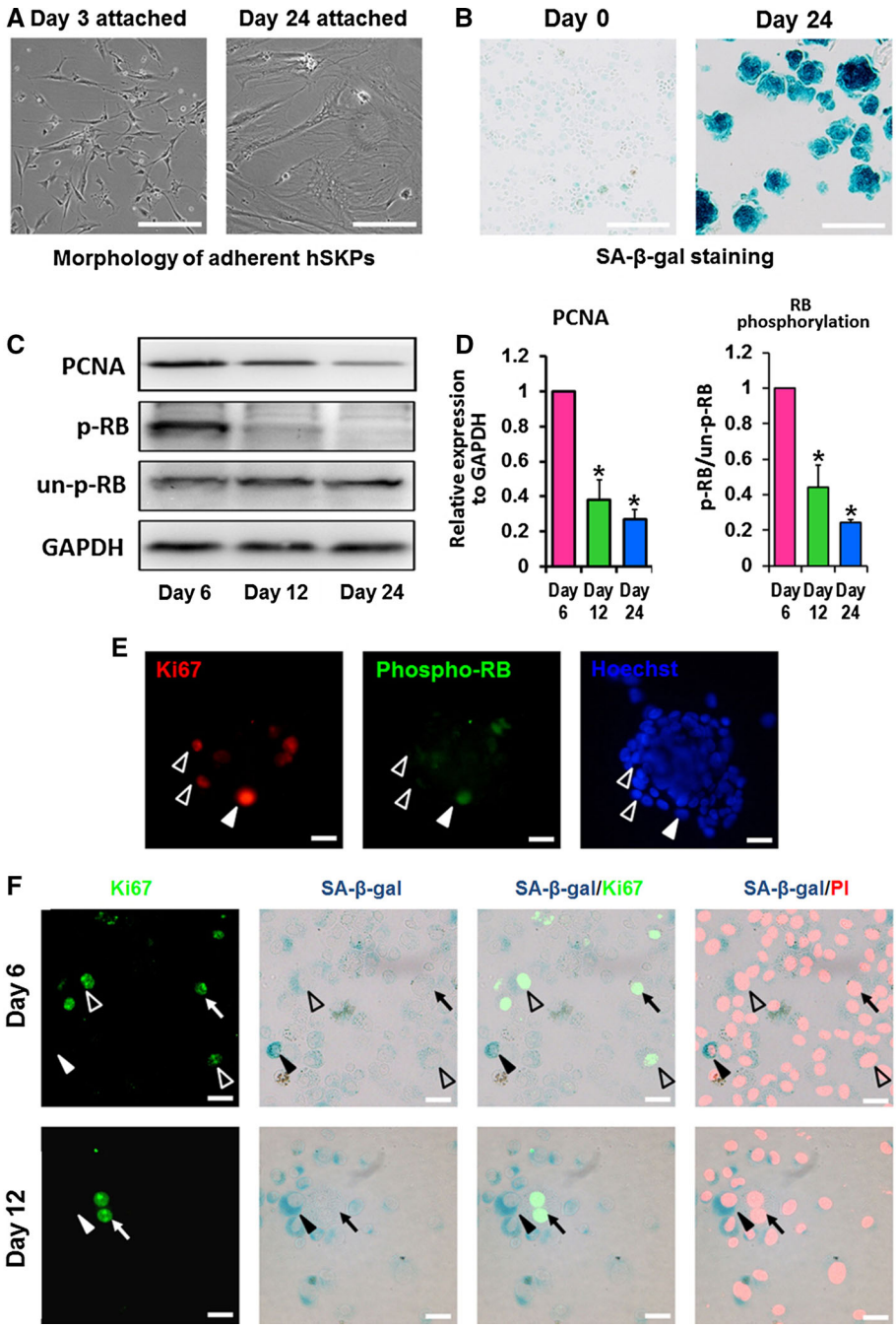

Fig. 1 The senescent phenotype of hSKPs. **a** Morphology of attached hSKPs on Day 3 and 24 of routine culture. **b** SA-β-gal staining of freshly isolated human dermal cells (*left*) and Day 24 hSKP spheres (*right*). **c** Western blots showing the expression of PCNA and phosphorylation of RB in hSKPs on different days of culture. **d** Statistical analysis of PCNA expression and RB phosphorylation in hSKPs according to grayscale images of western blots. **e** Immunofluorescence staining of Ki67 and p-RB in hSKPs. *Arrow heads* a Ki67+/p-RB+ cell and *hollow arrow heads* Ki67+/p-RB− cells. **f** Costaining of Ki67 and SA-β-gal in hSKPs on Day 6 and 12. *Arrows* Ki67+/SA-β-gal− cells; *arrow heads* Ki67-/SA-β-gal+ cells; *hollow arrow heads* Ki67+/SA-β-gal+ cells. *p-RB* phosphorylated RB. *Scale bar* 100 μm in **a** and **b**; *scale bar* 20 μm in **e** and **f**

(Fig. 2c). Details of genes in each profile are listed in Table S2. Molecular function clustering showed that most significant categories in both up-regulated (red) and down-regulated (green) genes were protein binding, ion binding and receptor activity (Fig. 2d, left panel). Top categories of biological process in down-regulated genes included those related to cell cycle (Fig. 2d, mid panel, bottom), consistent with the cell cycle arrest phenotype in hSKPs. Among up-regulated genes, top biological process categories included cell adhesion, signal transduction and ion transport (Fig. 2d, mid panel, top), which might be associated with the altered metabolism of senescent cells. Complete gene ontology (GO) term list is shown in Table S3. To our surprise, many reported cellular senescence-associated genes, especially those concerning the senescence-associated secretory phenotype (SASP), did not show an accordant variation (Table S4). Thus, we speculate that hSKP senescence has its unique phenotype and mechanisms.

We looked into cyclin-dependent kinase inhibitor (CDKI) genes which functioned in G1 phase and G1 to S

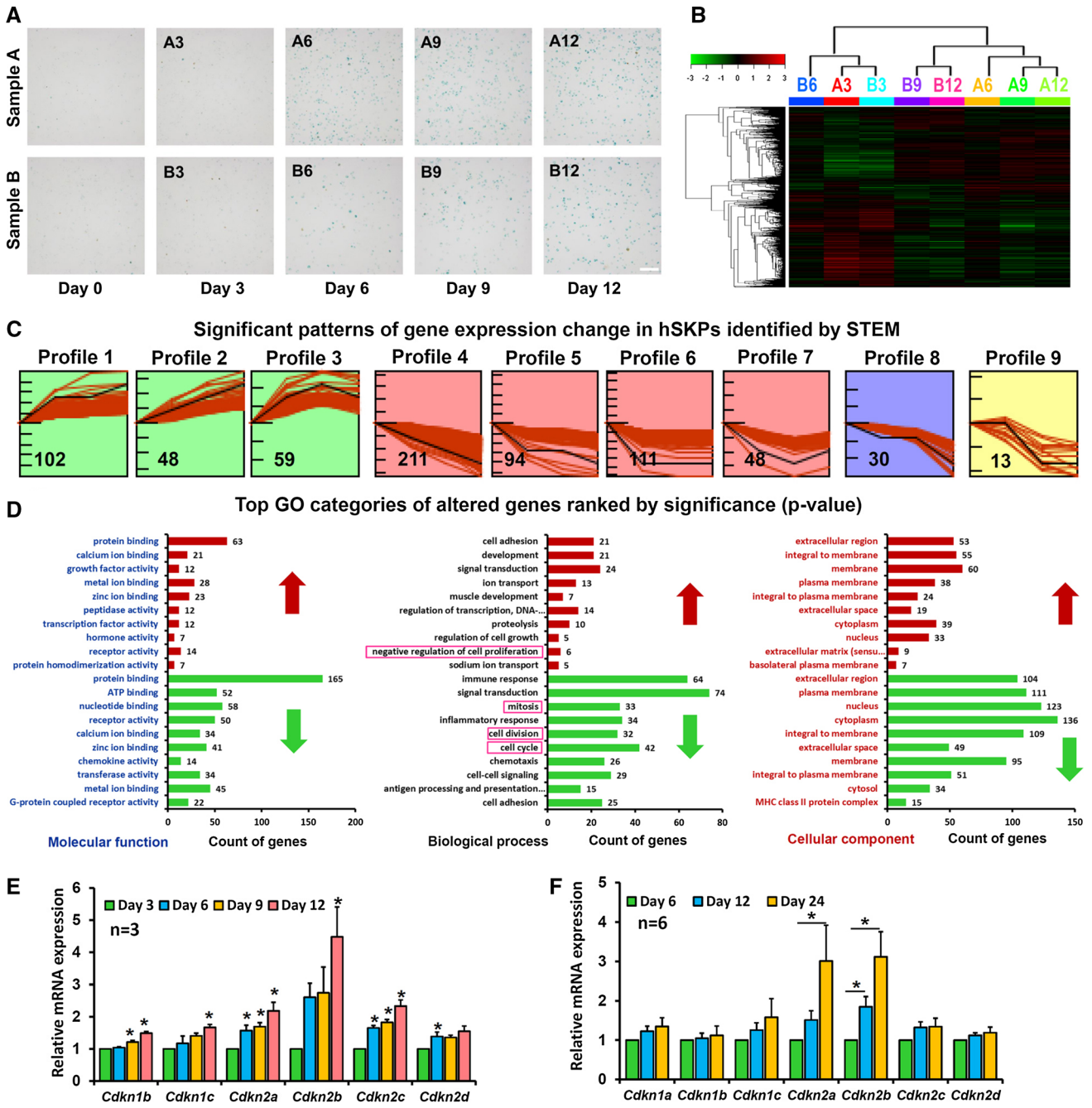

Fig. 2 Microarray analysis of hSKPs. **a** SA-β-gal staining of hSKPs from two individual donors used in microarray experiments on different days of culture. *Symbols* in the *top left corners* of the *picture* stand for different sample name in microarray experiments. *Scale bar* 100 μm. **b** Clustering of different samples according to their gene expression profiles. **c** Significant patterns of gene expression change in hSKPs identified by STEM software. Each *box* corresponds to a model expression profile. *Black lines* are the model expression profile and *red lines* are the actual expression profile of different genes. The *number* in the *bottom left corner* of each *box* stands for number of genes in each model. **d** Top GO categories of altered genes ranked by significance (*p* value). **e** qPCR analysis of CDKI gene expression in hSKPs from three donors during the first 12 days of culture. **f** qPCR analysis of CDKI gene expression in hSKPs from six donors during the first 24 days of culture

progression. Microarray data indicated an obvious expression increase of *Cdkn2b* (Table S1). qPCR analysis showed an overall significant up-regulation of *Cdkn1b*, *Cdkn1c*, *Cdkn2a*, *Cdkn2b*, *Cdkn2c* and *Cdkn2d* mRNA during the first 12 days, despite the small fold change for several genes (*Cdkn1b*, *Cdkn1c* and *Cdkn2d*) (Fig. 2e). *Cdkn1a* expression level on Day 3 was too low to be accurately determined, and *Cdkn2d* mRNA level was also very low. In

prolonged culture, only *Cdkn2a* and *Cdkn2b* levels kept rising (Fig. 2f), suggesting possible involvement of these CDKIs in hSKP senescence.

Cdkn2a encodes $p16^{INK4a}$ and $p14^{ARF}$ proteins, both involved in cell cycle regulation. $p14^{ARF}$ mainly acts on p53 pathway, a key regulator of DNA damage responses and cellular senescence [17]. $p16^{INK4a}$ itself is also another key regulator in cellular senescence induced by insults other than DNA damage [17]. *Cdkn2b* encodes $p15^{INK4b}$, which is also reported to function in cellular senescence. We next examined possible mechanisms related to the above CDKIs.

hSKP senescence is not activated by DNA damage and p53 pathway

p53 signaling is one of the most important two pathways in cellular senescence, which is usually induced by stimuli that generate DDR such as radiation, oxidative stress, telomere dysfunction. With GO analysis of our microarray data (Table S3), we noted that some genes related to oxidative stress and DDR showed significant change in hSKPs. Therefore, we looked into this possibility. Histone H2A.x phosphorylated at Ser139 (γH2A.X) is a biomarker of double strand break (DSB) of DNA. There were indeed a few hSKPs with DSB, as indicated by their focal staining of γH2A.X (Fig. 3a). γH2A.X+ and Ki67+ cells were largely non-overlapping (hollow arrow heads in Fig. 3a), but there were cells with DSB still proliferating (arrow heads in Fig. 3a), suggesting that growth arrest had not been triggered in these cells yet. Flow cytometry showed no significant change in γH2A.X fluorescence among hSKPs on different days of culture (Fig. 3b), indicating relatively consistent small portion of cells with DSB.

In line with the low level of DSB in hSKPs, p53 expression was found in only a minority of hSKPs (Fig. 3c) and showed only a slight increase with time (Fig. 3d). p53+ cells generally showed no proliferation, with only a minor exception (arrows in Fig. 3c). $p21^{CIP1}$, the effector of p53, showed similar expression pattern to p53 (Fig. 3e), and its mRNA level had no significant change during culture (*Cdkn1a*, Fig. 2f). We compared mRNA levels of $p21^{CIP1}$ in hSKPs and fibroblasts (hFbs) from the same donors. Interestingly, Day 12 and 24 $p21^{CIP1}$ mRNA levels in hSKPs were comparable with those in hFbs, which showed no senescence or growth arrest (Fig. 3f), suggesting that $p21^{CIP1}$ level in hSKPs was not sufficient to induce senescence. Further verification was performed by efficient p53 knockdown in hSKPs (Fig. 3g), which had no effect on hSKP senescence (Fig. 3h), ruling out p53 and $p21^{CIP1}$ as hSKP senescence effectors.

hSKP senescence is not mediated by $p16^{INK4a}$

We previously reported an increase of $p16^{INK4a}$ protein in hSKPs in culture and a prominent $p16^{INK4a}$ expression in hSKPs on Day 24 [8]. Here, qPCR results pointed to an up-regulation of *Cdkn2a* gene expression with time, but the fold change was small during the first 12 days (Fig. 2e, f). On Day 12, however, there were already a considerable portion of senescent cells. Thus, we compared $p16^{INK4a}$ expression with SA-β-gal staining. On Day 6, when neither $p16^{INK4a}$ expression nor senescence was prominent, $p16^{INK4a}$ and SA-β-gal staining showed little relevance, with only a few cells positive for both markers (Fig. 3i, top). On Day 18, with both $p16^{INK4a}$+ and SA-β-gal+ populations expanded, double positive cells also increased (Fig. 3i, bottom). The existence of SA-β-gal+ cells without $p16^{INK4a}$ expression suggested a mechanism independent of $p16^{INK4a}$. Also, non-senescent hFbs showed similar increase in $p16^{INK4a}$ mRNA levels with time (Fig. 3j). Knocking down $p16^{INK4a}$ in hSKPs failed to alleviate senescence, as expected (Fig. 3k, l). Therefore, hSKPs senescence was not mediated by $p16^{INK4a}$, either.

$p15^{INK4b}$ and $p27^{KIP1}$ are involved in hSKP senescence

We compared the expression of *Cdkn2b* in hSKPs and hFbs from the same donors. As shown in Fig. 4a, *Cdkn2b* expression in hSKPs increased with time and was three- to five-fold higher than that in hFbs, suggesting a possible involvement of $p15^{INK4b}$ in hSKP senescence. We also checked $p15^{INK4b}$ protein level in hSKPs, which showed a consistent up-regulation with time (Fig. 4b). However, costaining of $p15^{INK4b}$ and Ki67 indicated that most proliferative cells (Ki67+) showed $p15^{INK4b}$ expression (Fig. 4c), suggesting no direct inhibition of proliferation by $p15^{INK4b}$. We also did RNAi to knockdown $p15^{INK4b}$ in hSKPs. While all 3 RNAi vectors worked well at mRNA level (Fig. 4d), only two of them had an obvious knockdown effect at protein level (Fig. 4e). These two groups showed moderately alleviated SA-β-gal staining, indicating reduced cellular senescence (Fig. 4f, g). Accordingly, these two groups showed enhanced expression of proliferation marker PCNA (Fig. 4e).

Since $p15^{INK4b}$ had no direct inhibition of hSKP proliferation and its knockdown only slightly alleviated hSKP senescence, we speculated that other CDKI(s) might still play a role. We noticed that although the expression level of *Cdkn1b* (encoding $p27^{KIP1}$) showed no uniform variation tendency in different samples, its expression signals are stronger than other CDKIs (Table S1). Interestingly, $p27^{KIP1}$ and Ki67 staining were absolutely exclusive of each other (Fig. 4h), indicating that $p27^{KIP1}$+ cells were non-proliferative. To examine the contribution of $p27^{KIP1}$ to

hSKP senescence, we knocked it down in hSKPs. Two out of three shRNA vectors showed significant knockdown effect (Fig. 4i, j). $p27^{KIP1}$-deficient hSKPs showed significantly reduced SA-β-gal staining (Fig. 4k, l) and increased PCNA expression (Fig. 4j). Therefore, our results demonstrate that $p27^{KIP1}$ plays a role in hSKP senescence.

AKT hypo-activity and insufficient inhibition of FOXO3 contribute to hSKP senescence

We next looked into the upstream regulators of $p15^{INK4b}$ and $p27^{KIP1}$ in cell cycle control. Both CDKIs were regulated by FOXO3, whose immunostaining in hSKPs at different time points revealed its presence in the majority of cells and a predominant nuclear location (Fig. 5a), indicating a continuous activity. Costaining of FOXO3 and Ki67 indicated that some FOXO3-active cells were still proliferative (arrow heads in Fig. 5a). Lentiviral RNAi of FOXO3 in hSKPs showed effective knockdown of FOXO3 protein (Fig. 5b, e), together with significantly decreased SA-β-gal staining (Fig. 4c). SA-β-gal+ cells on Day 13 dropped around 50 % in FOXO3 knockdown groups (Fig. 4d). FOXO3 knockdown inhibited $p15^{INK4b}$ and $p27^{KIP1}$ expression, and increased proliferation marker PCNA expression (Fig. 4e).

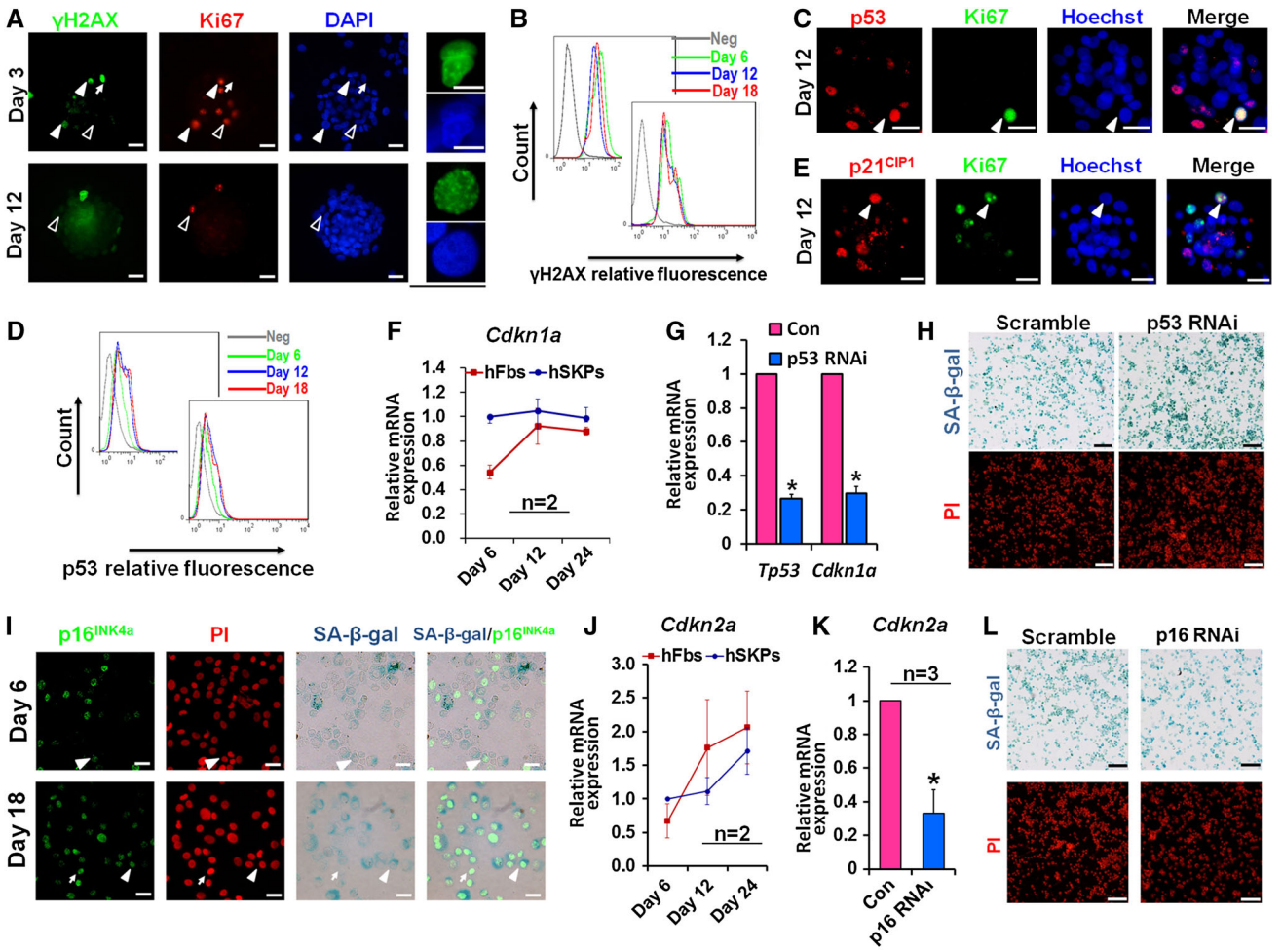

Fig. 3 DNA damage, p53 and $p16^{INK4a}$ in hSKP senescence. **a** Costaining of γH2AX and Ki67 in hSKPs on Day 3 and 12. *Arrows* a γH2AX+/Ki67− cell; *arrow heads* γH2AX+/Ki67+ cells; *hollow arrow heads* γH2AX-/Ki67+ cells. **b** Flow cytometric analysis of γH2AX expression in hSKPs from two independent donors on different days of culture. **c** Costaining of p53 and Ki67 in hSKPs on Day 12. *Arrow heads* a p53+/Ki67+ cell. **d** Flow cytometric analysis of p53 expression in hSKPs from two independent donors on different days of culture. **e** Costaining of $p21^{CIP1}$ and Ki67 in hSKPs on Day 12. *Arrow heads* a $p21^{CIP1}$+/Ki67+ cell. **f** qPCR analysis of *Cdkn1a* relative gene expression in hSKPs (*blue*) and hFbs (*red*) from the same two independent donors. **g** qPCR analysis of *Tp53* and *Cdkn1a* relative expression in hSKPs with or without p53 RNAi. **h** SA-β-gal staining and PI counter-staining of hSKPs with or without p53 RNAi. **i** Costaining of $p16^{INK4a}$ and SA-β-gal in hSKPs on Day 6 and 18. *Arrows* a $p16^{INK4a}$+/SA-β-gal− cell and *arrow heads* $p16^{INK4a}$+/SA-β-gal+ cells. **j** qPCR analysis of *Cdkn2a* relative gene expression in hSKPs (*blue*) and hFbs (*red*) from the same two independent donors. **k** qPCR analysis of *Cdkn2a* relative expression in hSKPs with or without $p16^{INK4a}$ RNAi. **l** SA-β-gal staining and PI counter-staining of hSKPs with or without $p16^{INK4a}$ RNAi. *Scale bar* 20 μm in **a**, **c**, **e** and **i**; *scale bar* 100 μm in **h** and **l**

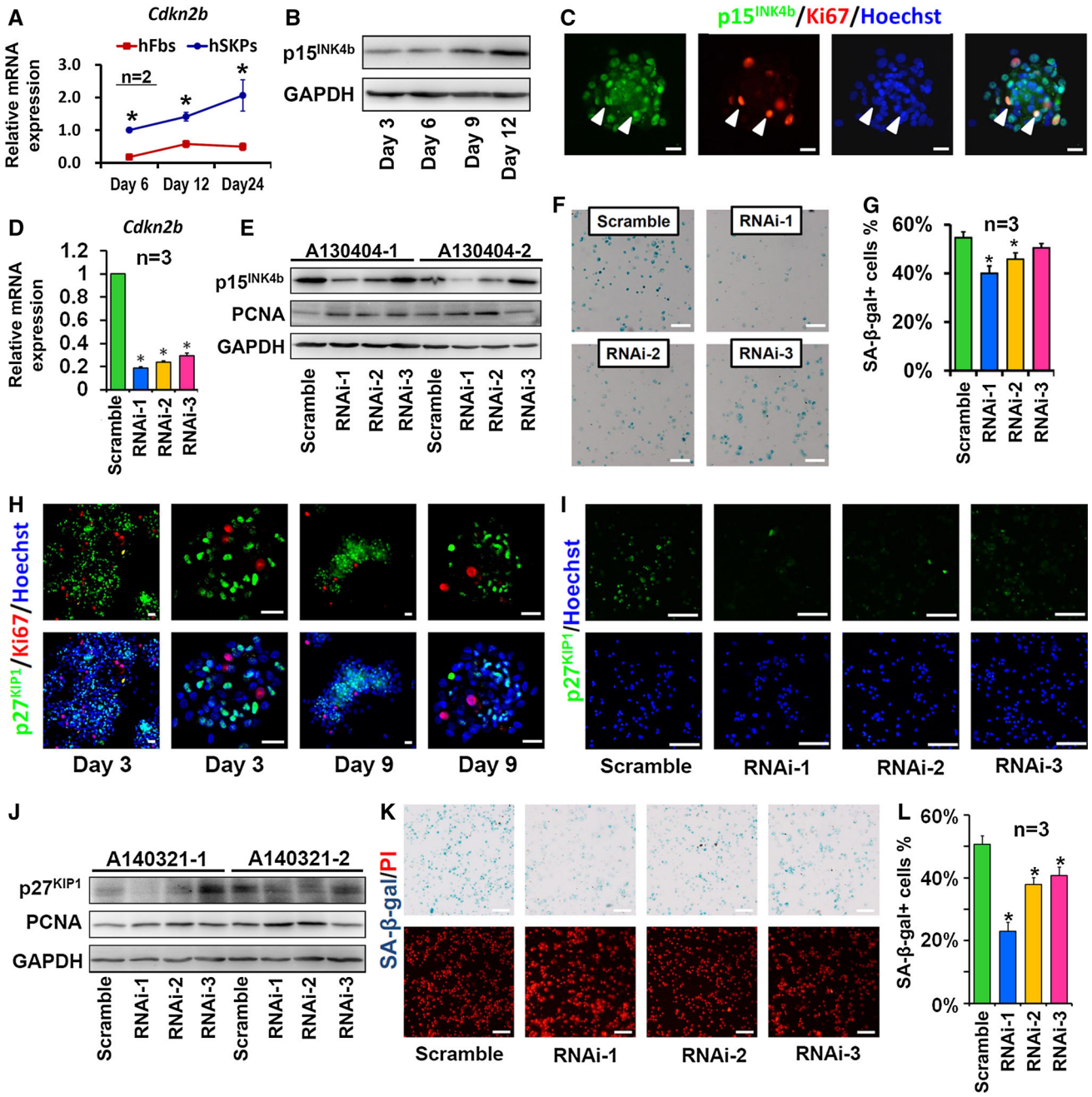

Fig. 4 p15^{INK4b} and p27^{KIP1}in hSKP senescence. **a** qPCR analysis of *Cdkn2b* relative gene expression in hSKPs (*blue*) and hFbs (*red*) from the same two independent donors. The expression difference at each time point is significant between hSKPs and hFbs. **b** Western blot analysis of p15^{INK4b} and GAPDH (loading control) expression in hSKPs on different days of culture. **c** Costaining of p15^{INK4b} and Ki67 in hSKPs. *Arrow heads* p15^{INK4b}+/Ki67+ cells. **d** qPCR analysis of *Cdkn2b* relative expression in hSKPs with or without p15^{INK4b} RNAi. **e** Western blots showing p15^{INK4b} and PCNA protein expression in hSKPs from two donors with or without p15^{INK4b} RNAi. **f** SA-β-gal staining of hSKPs with or without p15^{INK4b} RNAi. **g** Statistical analysis of SA-β-gal+ cell percentage in **f**. **h** Costaining of p27^{KIP1} and Ki67 in hSKPs on Day 3 and 9. **i** p27^{KIP1} staining and Hoechst counter-staining in hSKPs with or without p27^{KIP1} RNAi. **j** Western blots showing the expression of p27^{KIP1} and PCNA protein in hSKPs from two donors with or without p27^{KIP1} RNAi. **k** SA-β-gal staining and PI counter-staining of hSKPs with or without p27^{KIP1} RNAi. **l** Statistical analysis of SA-β-gal+ cell percentage in hSKPs with or without p27^{KIP1} RNAi. *Scale bar* 20 μm in **c** and **h**; *scale bar* 100 μm in **f, i** and **k**

FOXO3 is phosphorylated and inhibited by protein kinase B (Akt), whose maximal activity depends on the phosphorylation at both Ser473 and Thr308 sites. We previously found that Akt phosphorylation at Ser473 (p-Akt 473) in hSKPs decreased with time [8]. Here, we further checked the phosphorylation status of Thr308 (p-

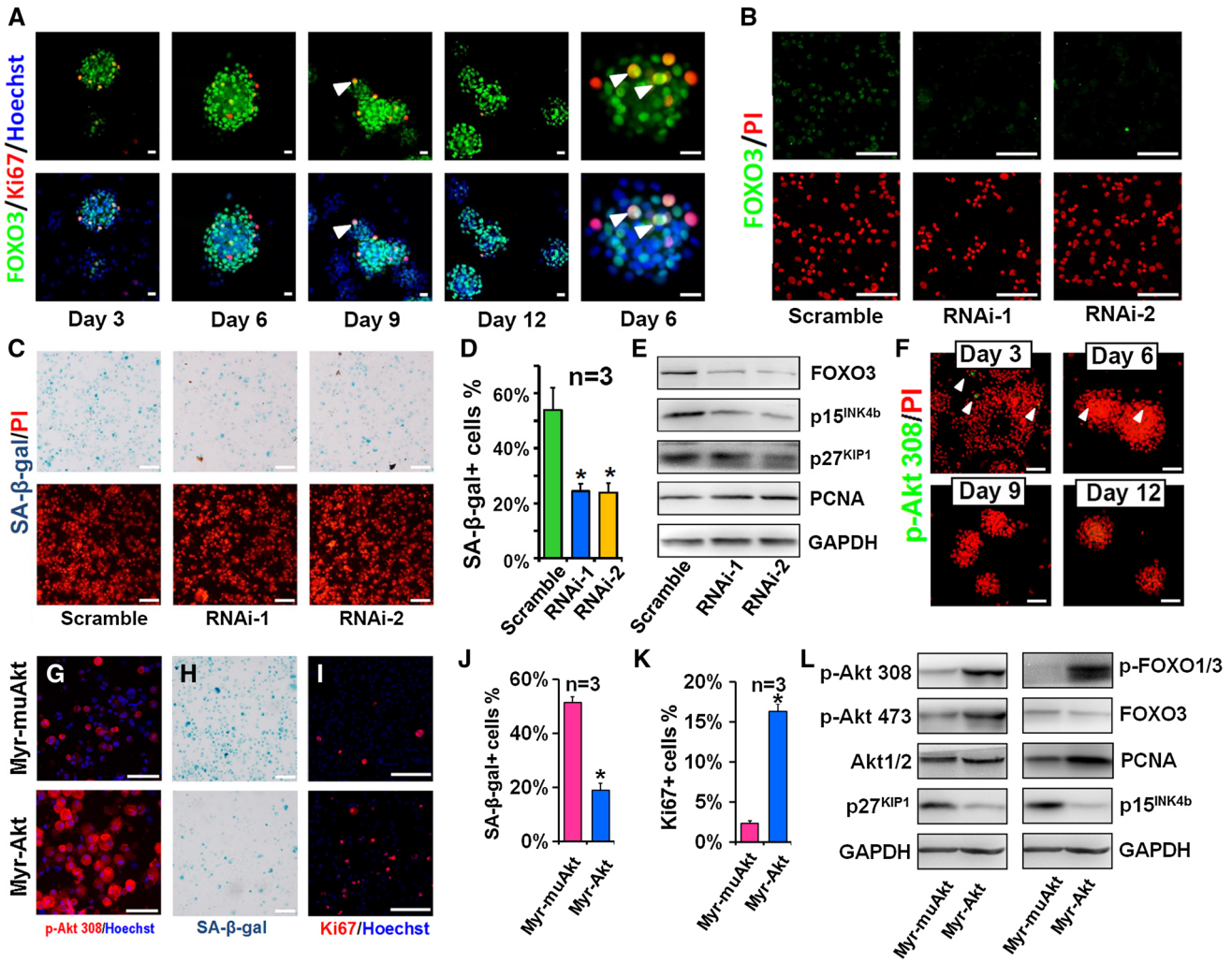

Fig. 5 FOXO3 and Akt in hSKP senescence. **a** Costaining of FOXO3 and Ki67 in hSKPs on different days of culture. *Arrow heads* FOXO3+/Ki67+ cells. **b** FOXO3 and Hoechst staining in hSKPs with or without FOXO3 RNAi. **c** SA-β-gal and PI staining of hSKPs with or without FOXO3 RNAi. **d** Statistical analysis of SA-β-gal+ cell percentage in hSKPs with or without FOXO3 RNAi. **e** Western blots showing the expression of FOXO3, $p15^{INK4b}$, $p27^{KIP1}$, PCNA and GAPDH (loading control) protein expression in hSKPs with or without FOXO3 RNAi. **f** Immunofluorescence staining of p-Akt 308 in hSKPs at different days of culture. Staining of p-Akt 308 (**g**), SA-β-gal (**h**) and Ki67 (**i**) in hSKPs introduced with Myr-muAkt (*top*) and Myr-Akt (*bottom*). SA-β-gal+ (**j**) and Ki67+ (**k**) cell percentages in hSKPs introduced with Myr-muAkt (*pink*) and Myr-Akt (*blue*). **l** Western blots showing the expression of p-Akt 308, p-Akt 473, Akt1/2, p-FOXO1/3, FOXO3, $p27^{KIP1}$, $p15^{INK4b}$, PCNA and GAPDH proteins in hSKPs introduced with Myr-muAkt and Myr-Akt. *Scale bar* 20 μm in **a**; *scale bar* 100 μm in **b**, **c**, **f**–**i**

Akt 308) in hSKPs on different days. To our surprise, very few cells were positive for p-Akt 308, even at the early stage of culture (Fig. 4f). Western blot assay indicated consistent results (Fig. S3a). However, in hFbs, bands for p-Akt 308 were clear on any analyzed days (Fig. S3b). In summary, hSKPs had inadequate Akt activation from the very beginning, which possibly led to the strong activity of FOXO3.

We previously used several growth factors such as PDGF to activate Akt in hSKPs [8]. Because our microarray data indicated significant change in the expression of several genes related to the IGF pathway, here we used the combination of different doses of IGF-1 and IGF-2 to try to activate Akt (Fig. S4a). However, IGF treatments failed to phosphorylate Akt at Thr308 and inhibit FOXO3 nuclear localization (Fig. S4b, first and second rows). hSKP proliferation was only slightly promoted with the highest concentrations of IGF (Fig. S4b, third row and Fig. S4c), and hSKP senescence was not changed by IGF treatments (Fig. S4b, last row).

To fully activate Akt and access its role in hSKP senescence, we introduced into hSKPs constitutively active Myr-Akt using lentiviral vectors. Myr-Akt expressing hSKPs showed substantial Akt phosphorylation at both sites (Fig. 5i; Fig. S5). Immunostaining also showed the expression of p-Akt 308 in the vast majority of hSKPs after

Myr-Akt introduction (Fig. 5g). Compared with mutated Myr-Akt control which did not have activity, Myr-Akt-hSKPs showed a significant decrease in SA-β-gal+ cell ratio (Fig. 5h, j) and an increase in Ki67+ cell ratio (Fig. 5i, k), indicating an inhibition of cellular senescence and a promotion of cell proliferation. We also checked downstream effectors after Akt activation in hSKPs. As expected, FOXO3 phosphorylation was up-regulated, and both $p15^{INK4b}$ and $p27^{KIP1}$ were down-regulated, compared with the mutated control (Fig. 5l). Also, the promotion of cell proliferation was further demonstrated by PCNA expression (Fig. 5l).

hSKP senescence is not mediated by GSK3β, mTOR or TGF-β signals

In addition to FOXOs, Akt also phosphorylates and inhibits GSK3β. In contrast to FOXO3, the phosphorylation of GSK3β (p-GSK3β) in hSKPs was robust in hSKPs (Fig. S6a), possibly because of other signals. Addition of GSK3β inhibitors CHIR99021 and BIO could no longer up-regulate its phosphorylation and inhibit its activity (Fig. S6b). As expected, CHIR99021 and BIO showed no effect on hSKP senescence (Fig. S6c). Besides, mTOR is an import downstream signal which is activated by Akt and plays important roles in cellular growth and organismal aging. We used two chemical compounds Propranolol and MHY1485 to further activate mTOR in hSKPs [18, 19]. Both activators showed obvious and specific activation of mTOR, indicated by phosphorylation of S6K (p-S6K) and further inhibition by Rapamycin (Fig. S6d). Neither the mTOR activator MHY1485 nor the inhibitor Rapamycin showed any effect on hSKP senescence (Fig. S6e). Although Propranolol treatment alleviated hSKP senescence, the effect could not be reversed by Rapamycin, indicating that the effect of Propranolol was mediated by other unknown signal instead of mTOR. Other than Akt, TGF-β also regulates $p15^{INK4b}$ in G1 arrest. We used SB431542 to inhibit TGF-β activity, indicated by Smad2/3 phosphorylation (p-Smad2/3) (Fig. S6f). We found that hSKP proliferation was enhanced upon TGF-β inhibition (Fig. S6g, h), cellular senescence was not altered (Fig. S6g), suggesting that TGF-β regulates hSKP proliferation but not senescence.

Discussion

In the present study, we investigated the senescence-specific gene expression profile of hSKPs and revealed the role of Akt-FOXO3-$p27^{KIP1}$/$p15^{INK4b}$ signaling in regulating hSKP senescence. The first surprising finding is that, although the hSKP senescence was also characterized by enlargement in cell volume, positive staining of SA-β-gal and decrease in RB phosphorylation and cell proliferation, it showed considerable differences with classical cellular senescence that has been reported. For example, senescence-associated heterochromatin foci (SAHF) which are domains of facultative heterochromatin often detected in senescent human cells by dense DAPI staining [20] were rarely seen in hSKP nuclei, even when there were many SA-β-gal+ cells (Fig. 3a). It is reported that the presence of SAHF in senescent cells depends on cell types and insults, and follows the expression of $p16^{INK4a}$ [21]. hSKP senescence was not mediated by $p16^{INK4a}$, and the up-regulation of $p16^{INK4a}$ lagged behind the emergence of senescent cells. This could possibly explain the rare presence of SAHF in hSKPs. We also compared the changes in gene expression with reported senescence-related gene expression profiles. Senescent cells secrete numerous pro-inflammatory cytokines, chemokines, growth factors, and proteases, a conserved feature of individual cell types called senescence-associated secretary phenotype (SASP) [11, 22]. As listed in Table S4, some of the genes (*Il13*, *Ccl16*, *Ccl25*, etc.) were absent in hSKPs; some of the genes (*Fgf2*, *Vegf*, *Il6*, etc.) did not show an increase in senescent hSKPs as in other senescent cell types. It is reported that SASP only occurs in senescent cells with DNA damage [22]. We demonstrated that hSKP senescence was not triggered by DNA damage. Therefore, it is reasonable that hSKP senescence did not show typical SASP but had its unique gene expression profile.

In accordance with the non-classical senescent phenotype of hSKPs, the regulatory mechanism of hSKP senescence also had its specificity. In our previous report, we speculated that hSKP senescence might be mediated by $p16^{INK4a}$ rather than p53. With a closer examination of $p16^{INK4a}$ expression, we found that its up-regulation was slower than the emergence of SA-β-gal+ cells, and the knockdown experiments further ruled out $p16^{INK4a}$ as a mediator of hSKP senescence. After examination of various CDKIs, we found a role of $p27^{KIP1}$ and $p15^{INK4b}$ in hSKP senescence. The $p15^{INK4b}$ gene, like the $p16^{INK4a}$ gene, is located at the *INK4a-ARF-INK4b* locus, which is famous for its crucial role in both cellular senescence and tumor suppression [23]. As a CDK4/6 inhibitor, $p15^{INK4b}$ overexpression is sufficient to induce a cellular senescent phenotype in cultured primary cells of early passages [24], as well as in human tumor cells [25]. Moreover, $p15^{INK4b}$ up-regulation is responsible for the cellular senescence induced by oncogenic Ras and for the inhibition of cellular transformation [26]. The role of the CDK2 inhibitor $p27^{KIP1}$ in cellular senescence has been reported in some particular tumors in vivo. For example, $p27^{KIP1}$ induces senescence and inhibits cell proliferation and cancer progression in a prostate cancer model [27]. Besides, it is also

associated with *Vhl* loss-induced senescence in the kidney [28]. In vitro, $p27^{KIP1}$ is required for RB-mediated senescence in a human osteosarcoma cell line and mediates senescence-like growth arrest induced by PI3K inhibitors in mouse embryonic fibroblasts [29, 30]. Interestingly, in the present study, hSKP senescence is also associated with hypo-phosphorylation of RB, inadequate AKT activity and abundant $p27^{KIP1}$ expression.

Several upstream molecules control $p27^{KIP1}$ and $p15^{INK4b}$ in cell cycle progression. The transcription of both inhibitors is activated by the FOXO transcription factors [31, 32]. Transaction activity of FOXOs relies on its nuclear localization which is inhibited upon their phosphorylation by Akt kinase. The PI3K-Akt pathway mediates multiple aspects of cellular activities including senescence. Indeed, inhibition of PI3K-Akt pathway activity and constitutively activated FOXOs has been reported to induce cellular senescence [30, 33]. However, recent studies has pointed out that over-activation of Akt and deficiency of FOXO also lead to premature senescence and shortening of cellular life span [34, 35], which was related to various diseases and organismal aging [13]. In fact, different extent of changes in pathway activity determines totally different outcomes. While moderate down-regulation of Akt pathway leads to decelerated proliferation and delayed cellular depletion, strong inhibition usually causes sharp cease of cell proliferation of the cells. In the present study, we concluded that the extremely low level of Akt activity could not support the normal proliferation of hSKPs and results in quick senescence.

It is intriguing to know what causes the hypo-activity of Akt in hSKPs. Routine hSKP culture condition contains EGF, which is known to activate multiple signals including the PI3K-Akt pathway. We indeed detected considerable EGFR expression in hSKPs and no obvious decline with time (data not shown). We also tried other growth factors to activate Akt, including PDGF whose receptor was robustly expressed in hSKPs [8], IGF (Fig. S4), and some other factors and peptides, all seemed not effective. In the future, it is worth working to investigate the trigger of hSKP senescence, not only to understand more about how cellular senescence is initiated and regulated, but also to create an optimal culture condition for hSKPs and push them one more step forward from bench to beside.

Acknowledgments We thank Prof. Zengqiang Yuan at the Institute of Biophysics, Chinese Academy of Sciences for his kind help with shRNA vectors. We also thank Prof. Aaron Hsueh at the Stanford University Medical Center for his comments on this work. This work was supported by the Strategic Priority Research Program of the Chinese Academy of Sciences XDA 01010202 (to E.D.), the National Basic Research Program of China 2011CB710905 (to E.D.), the National Natural Science Foundation of China 31201099 (to Shuang L.) and the Strategic Priority Research Program of the Chinese Academy of Sciences XDA 04020202-20 (to E.D.).

Conflict of interest The authors state no conflict of interest.

References

1. Liu S, Zhang H, Duan E (2013) Epidermal development in mammals: key regulators, signals from beneath, and stem cells. Int J Mol Sci 14:10869–10895. doi:10.3390/ijms140610869
2. Biernaskie J, Paris M, Morozova O, Fagan BM, Marra M, Pevny L, Miller FD (2009) SKPs derive from hair follicle precursors and exhibit properties of adult dermal stem cells. Cell Stem Cell 5:610–623. doi:10.1016/j.stem.2009.10.019
3. Qiu Z, Miao C, Li J, Lei X, Liu S, Guo W, Cao Y, Duan EK (2010) Skeletal myogenic potential of mouse skin-derived precursors. Stem Cells Dev 19:259–268. doi:10.1089/scd.2009.0058
4. Lavoie JF, Biernaskie JA, Chen Y, Bagli D, Alman B, Kaplan DR, Miller FD (2009) Skin-derived precursors differentiate into skeletogenic cell types and contribute to bone repair. Stem Cells Dev 18:893–906. doi:10.1089/scd.2008.0260
5. Biernaskie J, Sparling JS, Liu J, Shannon CP, Plemel JR, Xie Y, Miller FD, Tetzlaff W (2007) Skin-derived precursors generate myelinating Schwann cells that promote remyelination and functional recovery after contusion spinal cord injury. J Neurosci 27:9545–9559. doi:10.1523/JNEUROSCI.1930-07.2007
6. Toma JG, McKenzie IA, Bagli D, Miller FD (2005) Isolation and characterization of multipotent skin-derived precursors from human skin. Stem Cells 23:727–737. doi:10.1634/stemcells.2004-0134
7. Gago N, Perez-Lopez V, Sanz-Jaka JP, Cormenzana P, Eizaguirre I, Bernad A, Izeta A (2009) Age-dependent depletion of human skin-derived progenitor cells. Stem Cells 27:1164–1172. doi:10.1002/stem.27
8. Liu S, Liu S, Wang X, Zhou J, Cao Y, Wang F, Duan E (2011) The PI3K-Akt pathway inhibits senescence and promotes self-renewal of human skin-derived precursors in vitro. Aging Cell 10:661–674. doi:10.1111/j.1474-9726.2011.00704.x
9. Wang X, Liu S, Zhao Q et al (2014) Three-dimensional hydrogel scaffolds facilitate in vitro self-renewal of human skin-derived precursors. Acta Biomater 10:3177–3187. doi:10.1016/j.actbio.2014.03.018
10. Campisi J (1997) The biology of replicative senescence. Eur J Cancer 33:703–709. doi:10.1016/S0959-8049(96)00058-5
11. Campisi J (2013) Aging, cellular senescence, and cancer. Annu Rev Physiol 75:685–705. doi:10.1146/annurev-physiol-030212-183653
12. Suzuki M, Boothman DA (2008) Stress-induced premature senescence (SIPS). J Radiat Res 49:105–112. doi:10.1269/jrr.07081
13. Minamino T, Miyauchi H, Tateno K, Kunieda T, Komuro I (2004) Akt-induced cellular senescence: implication for human disease. Cell Cycle 3:449–451. doi:10.4161/cc.3.4.819
14. Kuki S, Imanishi T, Kobayashi K, Matsuo Y, Obana M, Akasaka T (2006) Hyperglycemia accelerated endothelial progenitor cell senescence via the activation of p38 mitogen-activated protein kinase. Circ J 70:1076–1081. doi:10.1253/circj.70.1076
15. Chien Y, Scuoppo C, Wang X et al (2011) Control of the senescence-associated secretory phenotype by NF-κB promotes senescence and enhances chemosensitivity. Genes Dev 25:2125–2136. doi:10.1101/gad.17276711
16. Ernst J, Bar-Joseph Z (2006) STEM: a tool for the analysis of short time series gene expression data. BMC Bioinform 7:191. doi:10.1186/1471-2105-7-191
17. Ben-Porath I, Weinberg RA (2005) The signals and pathways activating cellular senescence. Int J Biochem Cell Biol 37:961–976. doi:10.1016/j.biocel.2004.10.013
18. Hornberger TA, Chu WK, Mak YW, Hsiung JW, Huang SA, Chien S (2006) The role of phospholipase D and phosphatidic

acid in the mechanical activation of mTOR signaling in skeletal muscle. Proc Natl Acad Sci USA 103:4741–4746. doi:10.1073/pnas.0600678103
19. Choi YJ, Park YJ, Park JY et al (2012) Inhibitory effect of mTOR activator MHY1485 on autophagy: suppression of lysosomal fusion. PLoS ONE 7:e43418. doi:10.1371/journal.pone.0043418
20. Zhang R, Chen W, Adams PD (2007) Molecular dissection of formation of senescence-associated heterochromatin foci. Mol Cell Biol 27:2343–2358. doi:10.1128/MCB.02019-06
21. Kosar M, Bartkova J, Hubackova S, Hodny Z, Lukas J, Bartek J (2011) Senescence-associated heterochromatin foci are dispensable for cellular senescence, occur in a cell type- and insult-dependent manner and follow expression of p16ink4a. Cell Cycle 10:457–468. doi:10.4161/cc.10.3.14707
22. Coppe J-P, Desprez P-Y, Krtolica A, Campisi J (2010) The senescence-associated secretory phenotype: the dark side of tumor suppression. Annu Rev Pathol 5:99–118. doi:10.1146/annurev-pathol-121808-102144
23. Gil J, Peters G (2006) Regulation of the INK4b-ARF-INK4a tumour suppressor locus: all for one or one for all. Nat Rev Mol Cell Biol 7:667–677. doi:10.1038/Nrm1987
24. McConnell BB, Starborg M, Brookes S, Peters G (1998) Inhibitors of cyclin-dependent kinases induce features of replicative senescence in early passage human diploid fibroblasts. Curr Biol 8:351–354. doi:10.1016/S0960-9822(98)70137-X
25. Fuxe J, Akusjärvi G, Goike HM, Roos G, Collins VP, Pettersson RF (2000) Adenovirus-mediated overexpression of p15INK4B inhibits human glioma cell growth, induces replicative senescence, and inhibits telomerase activity similarly to p16INK4A. Cell Growth Differ 11:373–384
26. Malumbres M, Pérez De Castro I, Hernández MI, Jiménez M, Corral T, Pellicer A (2000) Cellular response to oncogenic Ras involves induction of the Cdk4 and Cdk6 inhibitor p15 INK4b. Mol Cell Biol 20:2915–2925. doi:10.1128/mcb.20.8.2915-2925.2000
27. Majumder PK, Grisanzio C, O'Connell F et al (2008) A prostatic intraepithelial neoplasia-dependent p27Kip1 checkpoint induces senescence and inhibits cell proliferation and cancer progression. Cancer Cell 14:146–155. doi:10.1016/j.ccr.2008.06.002
28. Young AP, Schlisio S, Minamishima YA, Zhang Q, Li L, Grisanzio C, Signoretti S, Kaelin WG (2008) VHL loss actuates a HIF-independent senescence programme mediated by Rb and p400. Nat Cell Biol 10:361–369. doi:10.1038/ncb1699
29. Alexander K, Hinds PW (2001) Requirement for p27KIP1 in retinoblastoma protein-mediated senescence. Mol Cell Biol 21:3616–3631. doi:10.1128/mcb.21.11.3616-3631.2001
30. Collado M, Medema RH, Garcia-Cao I et al (2000) Inhibition of the phosphoinositide 3-kinase pathway induces a senescence-like arrest mediated by p27Kip1. J Biol Chem 275:21960–21968. doi:10.1074/jbc.M000759200
31. Medema RH, Kops GJ, Bos JL, Burgering BM (2000) AFX-like Forkhead transcription factors mediate cell-cycle regulation by Ras and PKB through p27kip1. Nature 404:782–787. doi:10.1038/35008115
32. Katayama K, Nakamura A, Sugimoto Y, Tsuruo T, Fujita N (2007) FOXO transcription factor-dependent p15INK4b and p19INK4d expression. Oncogene 27:1677–1686. doi:10.1038/sj.onc.1210813
33. Courtois-Cox S, Genther Williams SM, Reczek EE, Johnson BW, McGillicuddy LT, Johannessen CM, Hollstein PE, MacCollin M, Cichowski K (2006) A negative feedback signaling network underlies oncogene-induced senescence. Cancer Cell 10:459–472. doi:10.1016/j.ccr.2006.10.003
34. Nogueira V, Park Y, Chen C-C, Xu P-Z, Chen M-L, Tonic I, Unterman T, Hay N (2008) Akt determines replicative senescence and oxidative or oncogenic premature senescence and sensitizes cells to oxidative apoptosis. Cancer Cell 14:458–470. doi:10.1016/j.ccr.2008.11.003
35. Kyoung Kim H, Kyoung Kim Y, Song I-H, Baek S-H, Lee S-R, Hye Kim J, Kim J-R (2005) Down-regulation of a forkhead transcription factor, FOXO3a, accelerates cellular senescence in human dermal fibroblasts. J Gerontol A Biol Sci Med Sci 60:4–9. doi:10.1093/gerona/60.1.4